Journal of Applied Mechanics Vol.7,pp.1061-1068 (August 2004) JSCE

Free Surface Profile Analysis of Flows with Air-core Vortex

Tran Ngoc ANH *, Takashi HOSODA **

* PhD Student, Dept. of Urban Management, Kyoto Univ. , Sakyo-ku, Kyoto 606-8501
** Professor, Dept. of Urban Management, Kyoto Univ. (606-8501 Kyoto)

A 1D theoretical model based on the depth-averaged flow equations has been developed to calculate the variation of water depth of flow with air-core vortex at an intake. The use of curvilinear coordinate avoids invalidation of the Kelvin's theorem in the core of vortex, thus the conservation of circulation can be applied for whole flow. The results of calculation show the ability of the model in analyzing the water surface profile and in predicting the critical submergence for vertical intake.

Key words: *air-core vortex, water surface profile, depth averaged flow model*

1. Introduction

Air-core vortex formation at intakes is a significant hydraulic engineering problem in many situations. It occurs typically whenever the submergence is less than a critical value and causes some detrimental effects as reduction in intake discharge, resulting vibrations and noises as well as operational difficulties. Several approaches have been presented in the literature to deal with the problem of determination and prediction of critical submergence serving in design works. These approaches basically can be labeled as analytical models[1,2,3] and physical models [4,5,6,7,8].

Many analytical approaches have been presented in the literature in order to attain a theoretical view of the far-field velocity; the flow representation has not been defined so far by any comprehensive analytical analysis. The concept of simple Rankine vortex normally used in the basic equations [2,3] could not be applied for the case of air-entraining vortex. Trivellato et al [9] set the water surface equal to the stationary headwater while other experimental works only focus on the critical submergence. Consequently, these approaches could not be used to predict the water surface profile of flow with air core vortex.

In this paper, the water surface profile of a steady air core vortex flow into a vertical intake was derived through out a depth-averaged model of open channel flows over the 3-D curvilinear bottom plane using a generalized and body fitted coordinate system. The assumption of fully free air-core vortex in the new coordinate allowed us to use the Kelvin's theorem of the conservation of circulation for the whole flow field. The vortex was assumed axisymmetric and steady. The assumption of shallow water and kinetic boundary condition at water surface were also used. The equation describing water surface profile was derived and calculated results were compared to formula introduced by Orgaard [2].

The application's results showed us the ability of the model in analyzing the water surface profile and can be improved to simulate the flow structure of an air-core vortex.

2. Mathematical Modeling

2.1 Coordinate setting

To consider the vortex occurring at a cavity on the bottom surface (Fig. 1), the position of any point P was defined by three value of (ξ,η,ζ), where ξ,η define the position of P_0 (projection of P) on the bottom plane, and ζ is the distance from point P to that plane.

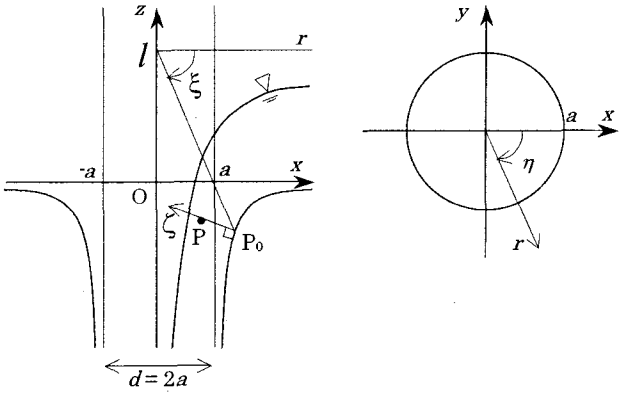

Fig. 1 Definition of coordinate components

Assuming that the shape of bottom surface (i.e at $\zeta = 0$) has the form of

$$z_0 = \frac{-b}{(r_0 - a)}, \tag{3}$$

where a and b are the coefficients which define the shape of the bottom as in fig. 1.

r_0 is the distance from a point on bottom to axis z: $r_0 = \sqrt{x_0{}^2 + y_0{}^2}$.

From eq. (3): $\dfrac{\partial z_0}{\partial r_0} = \dfrac{b}{(r_0 - a)^2}$

Refer to Fig. 1 we can get $x_0 = r_0 \cos\eta$ and $y_0 = -r_0 \sin\eta$.

Then, the bottom surface was expressed by the following equation:

$$\Phi(x_0, y_0, z_0) = (r_0 - a)z_0 + b = 0$$

The unit normal vector $(\vec{n})$ to the bottom surface was derived as:

$$\vec{n} = \frac{grad\Phi}{|grad\Phi|} = \frac{1}{\sqrt{z_0{}^2 + (r_0 - a)^2}} \frac{x_0 z_0}{r_0} \vec{i} + \frac{1}{\sqrt{z_0{}^2 + (r_0 - a)^2}} \frac{y_0 z_0}{r_0} \vec{j} + \frac{r_0 - a}{\sqrt{z_0{}^2 + (r_0 - a)^2}} \vec{k}$$

At $\zeta = \zeta$ the relations between (x, y, z) and (ξ, η, ζ) were expressed as:

$$x = x_0 + \frac{1}{\sqrt{z_0{}^2 + (r_0 - a)^2}} \frac{x_0 z_0}{r_0} \zeta = r_0 \cos\eta - \frac{b\cos\eta}{\sqrt{(r_0 - a)^4 + b^2}} \zeta \tag{4}$$

$$y = y_0 + \frac{1}{\sqrt{z_0{}^2 + (r_0 - a)^2}} \frac{y_0 z_0}{r_0} \zeta = -r_0 \sin\eta + \frac{b\sin\eta}{\sqrt{(r_0 - a)^4 + b^2}} \zeta \tag{5}$$

$$z = z_0 + \frac{r_0 - a}{\sqrt{z_0{}^2 + (r_0 - a)^2}} \zeta = -\frac{b}{(r_0 - a)} + \frac{(r_0 - a)^2}{\sqrt{(r_0 - a)^4 + b^2}} \zeta \tag{6}$$

Using equation (4)-(6), the covariant base vector components on the bottom surface were denoted as follows:

$$\vec{e_\xi} = x_{0\xi}\vec{i} + y_{0\xi}\vec{j} + z_{0\xi}\vec{k} = -\frac{\cos\eta}{p_1}\vec{i} + \frac{\sin\eta}{p_1}\vec{j} - \frac{b}{p_1(r_0 - a)^2}\vec{k}$$

$$\vec{e_\eta} = x_{0\eta}\vec{i} + y_{0\eta}\vec{j} + z_{0\eta}\vec{k} = -r_0 \sin\eta\vec{i} - r_0 \cos\eta_\eta \vec{j}$$

$$\vec{e_\zeta} = x_{0\zeta}\vec{i} + y_{0\zeta}\vec{j} + z_{0\zeta}\vec{k} = -\frac{b\cos\eta}{\sqrt{(r_0 - a)^4 + b^2}}\vec{i} + \frac{b\sin\eta}{\sqrt{(r_0 - a)^4 + b^2}}\vec{j} + \frac{(r_0 - a)^2}{\sqrt{(r_0 - a)^4 + b^2}}\vec{k} \tag{7}$$

and Jacobian right on the bottom plane is:

$$\frac{1}{J_0} = \begin{vmatrix} x_{\xi_0} & x_{\eta_0} & x_{\zeta_0} \\ y_{\xi_0} & y_{\eta_0} & y_{\zeta_0} \\ z_{\xi_0} & z_{\eta_0} & z_{\zeta_0} \end{vmatrix} = \frac{1}{p_1} \frac{r_0\sqrt{(r_0 - a)^4 + b^2}}{(r_0 - a)^2} \tag{8}$$

in which

$$p_1 = \frac{l(r_0 - a)^2 + b(r_0 - a) + br_0}{r_0{}^2(r_0 - a)^2 + l^2(r_0 - a)^2 + 2lb(r_0 - a) + b^2}$$

l is defined as in Fig. 1.

The Riemann-Christoffel symbol is defined as follows using the contravariant and covariant components of metric tensors:

$$\Gamma^i_{jk} = -\frac{\partial x^m}{\partial \xi^j}\frac{\partial}{\partial \xi^k}\left(\frac{\partial \xi^i}{\partial x^m}\right) \tag{9}$$

Using the equations (4)-(6), after some manipulation the value of Riemann-Chistoffel symbols on the bottom were derived as following:

$$\Gamma^{\xi}_{0\xi\eta} = \Gamma^{\xi}_{0\eta\xi} = \Gamma^{\zeta}_{0\eta\xi} = \Gamma^{\zeta}_{0\xi\eta} = 0 \tag{10}$$

2.2 Equation of water surface profile

The constant-density, incompressible continuity and momentum equations in a generalized curvilinear coordinate system were used.

Continuity equation:

$$\frac{\partial}{\partial\xi}\left(\frac{U}{J}\right) + \frac{\partial}{\partial\eta}\left(\frac{V}{J}\right) + \frac{\partial}{\partial\zeta}\left(\frac{W}{J}\right) = 0 \tag{11}$$

Momentum equation in ξ-component:

$$\frac{\partial}{\partial t}\left(\frac{U}{J}\right)+\frac{\partial}{\partial \xi}\left(\frac{U^2}{J}\right)+\frac{\partial}{\partial \eta}\left(\frac{VU}{J}\right)+\frac{\partial}{\partial \zeta}\left(\frac{WU}{J}\right)$$
$$+\frac{1}{J}\left(U^2\Gamma^{\xi}_{\xi\xi}+UV\Gamma^{\xi}_{\xi\eta}+UW\Gamma^{\xi}_{\xi\zeta}\right.$$
$$+VU\Gamma^{\xi}_{\eta\xi}+V^2\Gamma^{\xi}_{\eta\eta}+VW\Gamma^{\xi}_{\eta\zeta}+WU\Gamma^{\xi}_{\zeta\xi}+WV\Gamma^{\xi}_{\zeta\eta}$$
$$\left.+W^2\Gamma^{\xi}_{\zeta\zeta}\right)=\frac{G^{\xi}}{J}-(\text{pressure term})+\frac{\partial}{\partial \xi}\left(\frac{\tau^{\xi\xi}}{\rho J}\right)$$
$$+\frac{\partial}{\partial \eta}\left(\frac{\tau^{\xi\eta}}{\rho J}\right)+\frac{\partial}{\partial \zeta}\left(\frac{\tau^{\xi\zeta}}{\rho J}\right)+\frac{1}{\rho J}\left(\tau^{\xi\xi}\Gamma^{\xi}_{\xi\xi}+\tau^{\xi\eta}\Gamma^{\xi}_{\xi\eta}\right.$$
$$+\tau^{\xi\zeta}\Gamma^{\xi}_{\xi\zeta}+\tau^{\eta\xi}\Gamma^{\xi}_{\eta\xi}+\tau^{\eta\eta}\Gamma^{\xi}_{\eta\eta}+\tau^{\eta\zeta}\Gamma^{\xi}_{\eta\zeta}+\tau^{\zeta\xi}\Gamma^{\xi}_{\zeta\xi}$$
$$\left.+\tau^{\zeta\eta}\Gamma^{\xi}_{\zeta\eta}+\tau^{\zeta\zeta}\Gamma^{\xi}_{\zeta\zeta}\right) \qquad (12)$$

where:

$$(\text{pressure term})=\frac{1}{J}\left(\xi_x\xi_x+\xi_y\xi_y+\xi_z\xi_z\right)\frac{\partial}{\partial \xi}\left(\frac{p}{\rho}\right)$$
$$+\frac{1}{J}\left(\xi_x\eta_x+\xi_y\eta_y+\xi_z\eta_z\right)\frac{\partial}{\partial \eta}\left(\frac{p}{\rho}\right)$$
$$+\frac{1}{J}\left(\xi_x\zeta_x+\xi_y\zeta_y+\xi_z\zeta_z\right)\frac{\partial}{\partial \zeta}\left(\frac{p}{\rho}\right)$$
$$+\xi_x\frac{p}{\rho}\left\{\frac{\partial}{\partial \xi}\left(\frac{\xi_x}{J}\right)+\frac{\partial}{\partial \eta}\left(\frac{\eta_x}{J}\right)+\frac{\partial}{\partial \zeta}\left(\frac{\zeta_x}{J}\right)\right\}$$
$$+\xi_y\frac{p}{\rho}\left\{\frac{\partial}{\partial \xi}\left(\frac{\xi_y}{J}\right)+\frac{\partial}{\partial \eta}\left(\frac{\eta_y}{J}\right)+\frac{\partial}{\partial \zeta}\left(\frac{\zeta_y}{J}\right)\right\}$$
$$+\xi_z\frac{p}{\rho}\left\{\frac{\partial}{\partial \xi}\left(\frac{\xi_z}{J}\right)+\frac{\partial}{\partial \eta}\left(\frac{\eta_z}{J}\right)+\frac{\partial}{\partial \zeta}\left(\frac{\zeta_z}{J}\right)\right\}$$

in which (U,V,W) : the contravariant components of velocity vectors

J : Jacobian, $\frac{1}{J}=\begin{vmatrix} x_\xi & x_\eta & x_\zeta \\ y_\xi & y_\eta & y_\zeta \\ z_\xi & z_\eta & z_\zeta \end{vmatrix}$

Γ^{i}_{jk} : the Riemann-Christoffel symbols, $\Gamma^{i}_{jk}=-\frac{\partial x^m}{\partial \xi^j}\frac{\partial}{\partial \xi^k}\left(\frac{\partial \xi^i}{\partial x^m}\right)$, (m=1,2,3)

G^{ξ} , τ^{ξ} : the contravariant components of gravitational vector and shear stress vector acting on the bottom.

Assuming the shallow water condition, the value of Jacobian J can be approximately expressed as J_0 at $\zeta=0$ ($J_0=J|_{\zeta=0}$ as in eq. (8)) and U,V are uniform in ζ -direction, integrating eq. (11) with respect to the ζ -direction from the bottom to water surface, the depth averaged continuity equation was derived as:

$$\frac{\partial}{\partial \xi}\frac{M}{J_0}-\frac{U_S}{J_0}\frac{\partial h}{\partial \xi}+\frac{\partial}{\partial \eta}\frac{N}{J_0}-\frac{V_S}{J_0}\frac{\partial h}{\partial \eta}+\frac{W_S}{J_0}-\frac{W_B}{J_0}=0 \qquad (13)$$

Plugging equation (13) with the kinematic boundary at the free surface:

$$W_s=\frac{\partial h}{\partial t}+U_s\frac{\partial h}{\partial \xi}+V_s\frac{\partial h}{\partial \eta}$$

the continuity equation can be reduced as:

$$\frac{1}{J_0}\frac{\partial h}{\partial t}+\frac{\partial}{\partial \xi}\frac{M}{J_0}+\frac{\partial}{\partial \eta}\frac{N}{J_0}=0 \qquad (14)$$

in which $M=Uh$ and $N=Vh$, h is the depth of water flow in ζ -direction.

Integrating equation (12) with respect to the ζ -direction from the bottom to water surface, the momentum equation became:

$$\frac{\partial}{\partial t}\left(\frac{M}{J_0}\right)+\frac{\partial}{\partial \xi}\left(\frac{UM}{J_0}\right)+\frac{\partial}{\partial \eta}\left(\frac{VM}{J_0}\right)$$
$$+\frac{1}{J_0h}\left(M^2\Gamma^{\xi}_{0\xi\xi}+MN\Gamma^{\xi}_{0\xi\eta}+NM\Gamma^{\xi}_{0\eta\xi}+N^2\Gamma^{\xi}_{0\eta\eta}\right)$$
$$=\frac{h}{J_0}G^{\xi}-\frac{\xi^2_{x0}+\xi^2_{y0}+\xi^2_{z0}}{J_0}\frac{\partial}{\partial \xi}\int_0^h\frac{p}{\rho}d\zeta$$
$$-\frac{\xi_{x0}\eta_{x0}+\xi_{y0}\eta_{y0}+\xi_{z0}\eta_{z0}}{J_0}\frac{\partial}{\partial \eta}\int_0^h\frac{p}{\rho}d\zeta-\frac{\tau^{\xi}_b}{\rho J_0} \qquad (15)$$

with $\int_0^h\frac{p}{\rho}d\zeta=\left\{UU\Gamma^{\zeta}_{0\xi\xi}+VU\Gamma^{\zeta}_{0\eta\xi}+UV\Gamma^{\zeta}_{0\xi\eta}\right.$
$$\left.+VV\Gamma^{\zeta}_{0\eta\eta}-G^{\zeta}\right\}\frac{h^2}{2} \qquad (16)$$

Considering the steady status and the condition that the flow in the air-core vortex is axisymmetric, equation (14) and (15) became:

$$\frac{\partial}{\partial \xi}\frac{M}{J_0}=0 \text{ or } \frac{M}{J_0}=Q_0=const. \text{ or}$$

$$M=Q_0J_0 \qquad (17)$$

$$\frac{\partial}{\partial\xi}\left(\frac{UM}{J_0}\right)+\frac{1}{J_0 h}\left(M^2\Gamma_{0\xi\xi}^{\xi}+MN\Gamma_{0\xi\eta}^{\xi}+NM\Gamma_{0\eta\xi}^{\xi}\right.$$

$$\left.+N^2\Gamma_{0\eta\eta}^{\xi}\right)=\frac{h}{J_0}G^{\xi}-\frac{\xi_{x0}^2+\xi_{y0}^2+\xi_{z0}^2}{J_0}\frac{\partial}{\partial\xi}\left\{UU\Gamma_{0\xi\xi}^{\zeta}\right.$$

$$\left.+VU\Gamma_{0\eta\xi}^{\zeta}+UV\Gamma_{0\xi\eta}^{\zeta}+VV\Gamma_{0\eta\eta}^{\zeta}-G^{\zeta}\right)\frac{h^2}{2}\Bigg\}-\frac{\tau_b^{\xi}}{\rho J_0} \quad (18)$$

The model was developed by using the assumption of free vortex that was conservation of circulation $\Gamma=2\pi r_0 v$, where v is depth averaged tangential velocity at the cross-section r_0.

$v=r_0V^{\eta}\equiv r_0V$ thus $\Gamma=2\pi r_0^2V$ from which:

$$V=\frac{\Gamma}{2\pi r_0^2} \quad (19)$$

Substituting eq. (10), (17), (19), $M=Uh$ and $N=Vh$ into (18), it was yielded:

$$\frac{\partial}{\partial\xi}\left(\frac{Q_0^2J_0}{h}\right)+\frac{Q_0^2J_0}{h}\Gamma_{0\xi\xi}^{\xi}+\frac{\Gamma^2}{4\pi^2r_0^4}\frac{h}{J_0}\Gamma_{0\eta\eta}^{\xi}=$$

$$\frac{h}{J_0}G^{\xi}-\frac{\xi_{x0}^2+\xi_{y0}^2+\xi_{z0}^2}{J_0}\frac{\partial}{\partial\xi}\left\{\frac{Q_0^2J_0^2}{2}\Gamma_{0\xi\xi}^{\zeta}\right.$$

$$\left.+\frac{\Gamma^2}{4\pi^2r_0^4}\frac{h^2}{2}\Gamma_{0\eta\eta}^{\zeta}-\frac{h^2}{2}G^{\zeta}\right\}-\frac{\tau_b^{\xi}}{\rho J_0} \quad (20)$$

or

$$\left[\frac{\xi_{x0}^2+\xi_{y0}^2+\xi_{z0}^2}{J_0}\left\{\frac{\Gamma^2}{4\pi^2}h\frac{\Gamma_{0\eta\eta}^{\zeta}}{r_0^4}-G^{\zeta}h\right\}-\frac{Q_0^2J_0}{h^2}\right]\frac{\partial h}{\partial\xi}=$$

$$\frac{h}{J_0}G^{\xi}-\frac{Q_0^2}{h}\frac{\partial J_0}{\partial\xi}-\frac{Q_0^2J_0}{h}\Gamma_{0\xi\xi}^{\xi}-\frac{\Gamma^2}{4\pi^2r_0^4}\frac{h}{J_0}\Gamma_{0\eta\eta}^{\xi}$$

$$-\frac{\tau_b^{\xi}}{\rho J_0}-\frac{\xi_{x0}^2+\xi_{y0}^2+\xi_{z0}^2}{J_0}\left\{Q_0^2J_0\Gamma_{0\xi\xi}^{\zeta}\frac{\partial J_0}{\partial\xi}\right.$$

$$\left.+\frac{Q_0^2J_0^2}{2}\frac{\partial\Gamma_{0\xi\xi}^{\zeta}}{\partial\xi}+\frac{\Gamma^2}{8\pi^2}h^2\frac{\partial}{\partial\xi}\left(\frac{\Gamma_{0\eta\eta}^{\zeta}}{r_0^4}\right)-\frac{h^2}{2}\frac{\partial G^{\zeta}}{\partial\xi}\right\} \quad (21)$$

The evaluation of the contravariant component of shear stress acting on the bottom was computed using the following relation:

$$\frac{\tau_b^{\xi}}{\rho}=f|U|U=f|e_{\xi}|U^2 \Rightarrow \frac{\tau_b^{\xi}}{J_0\rho}=f\frac{Q_0^2}{r_0h^2} \quad (22)$$

where f is the resistant coefficient.

Substituting (22) into (21) then transforming special coordinates from ξ to r_0, after some manipulations we obtained the equation for water surface profile as:

$$\frac{\partial h}{\partial r_0}=-\frac{f_1(h,r_0)}{f_2(h,r_0)} \quad (23)$$

in which

$$f_1(h,r_0)=\left\{gb^2\frac{r_0^2(r_0-a)}{\left[(r_0-a)^4+b^2\right]^{3/2}}\right.$$

$$\left.-b\frac{\Gamma^2}{8\pi^2}\frac{3\left[(r_0-a)^4+b^2\right]+2r_0(r_0-a)^3}{r_0^2\left[(r_0-a)^4+b^2\right]^{3/2}}\right\}h^4$$

$$+\left\{\mathrm{gb}\frac{r_0^2}{(r_0-a)^2}-\frac{\Gamma^2}{4\pi^2}\frac{1}{r_0}\right\}h^3$$

$$+\left\{Q_0^2b\frac{2(r_0-a)^3}{r_0\left[(r_0-a)^4+b^2\right]^{3/2}}\right.$$

$$\left.+Q_0^2b\frac{3(r_0-a)^2\left[(r_0-a)^4-b^2\right]}{\left[(r_0-a)^4+b^2\right]^{5/2}}\right\}h^2$$

$$-\frac{Q_0^2}{r_0}h-f.Q_0^2\frac{\left[(r_0-a)^4+b^2\right]^{1/2}}{(r_0-a)^2} \quad (24)$$

$$f_2(h,r_0)=\frac{r_0^2(r_0-a)^2}{\left[(r_0-a)^4+b^2\right]^{1/2}}gh^3$$

$$+\frac{\Gamma^2}{4\pi^2}\frac{1}{r_0\left[(r_0-a)^4+b^2\right]^{1/2}}bh^3-Q_0^2 \quad (25)$$

3. Method of Calculation

The common method of analysis including singular point analysis was applied to calculate the water surface profile in both the upstream and downstream direction from this point. The singular point is defined as the point at which both functions $f_1(h,r_0)$ and $f_2(h,r_0)$ in equation (23) are equal to zero.

The equation $f_1(h,r_0)=0$ expresses the quasi-normal depth line whereas $f_2(h,r_0)=0$ expresses critical depth line (refer to Fig. 2).

The water surface was derived from eq. (23) by using Runge-Kutta scheme with the initial slope near the singular point defined by the following equation:

$$\left.\frac{dh}{dr_0}\right|_s=\frac{-\left(\left.\frac{\partial f_2}{\partial r_0}\right|_s+\left.\frac{\partial f_1}{\partial h}\right|_s\right)\pm\sqrt{\left(\left.\frac{\partial f_2}{\partial r_0}\right|_s+\left.\frac{\partial f_1}{\partial h}\right|_s\right)^2-4\left.\frac{\partial f_2}{\partial h}\right|_s\left.\frac{\partial f_1}{\partial r_0}\right|_s}}{2\left.\frac{\partial f_2}{\partial h}\right|_s}$$

(The subscript "s" was denoted for the derivatives taking at singular point.)

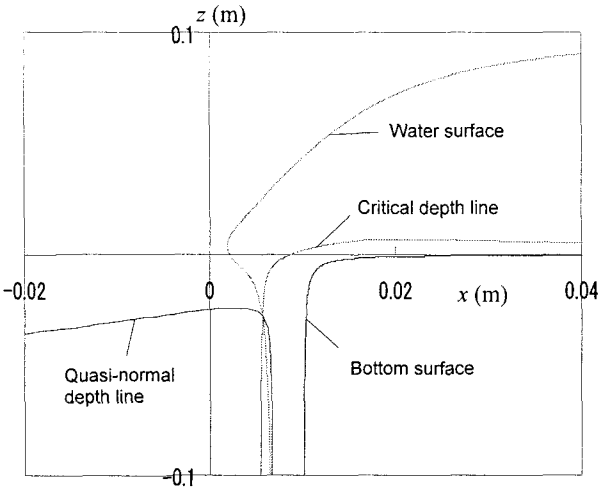

Fig. 2 An example of computed water surface profile with quasi-normal depth line and critical depth line.

4. Consideration of calculated results

The model has been applied in estimating water surface profile of flow with air-core vortex in different conditions.

Posey and Hsu [10], Jain et al [5] and others have reported that a large reduction in intake discharge was due to formation of vortices, especially in cases of flow entering the intake consisted of air. The model was applied with different imposed circulations (i.e. different strengths of vortex) and showed the reduction of discharge when the circulation increases while keeping the same submergence (water head) as in Fig. 3. It was observed that the larger circulation the deeper air core extends toward the intake, and in case of air-entrainment the discharge decreases until very low value (from 0.0015 to 0.0003 m^3/s), that is in agreement with the previous experiments [5,10]. Or in other words, intake discharge was inversely proportional to circulation as in Fig. 4 which the empty circles are calculated results and solid line is the trend line calculated by the least squares method.

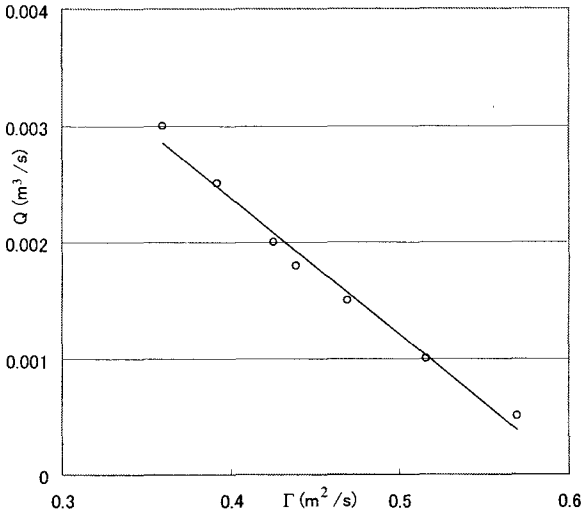

Fig. 4 Variation of intake discharge with circulation (a = 0.025m, b = 10^{-5} m^2, water head at the upstream end = 0.5m, f = 0.015)

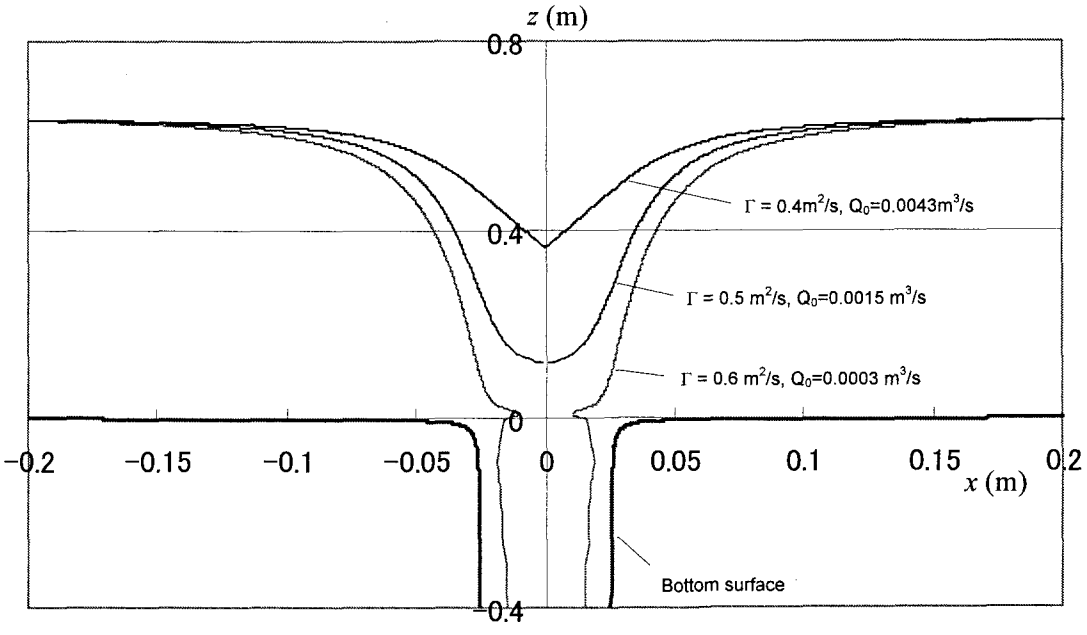

Fig. 3 The effect of circulation on water surface profile and intake discharge with the same water head (a = 0.025m, b=$10^{-5}$$m^2$, f =0.015)

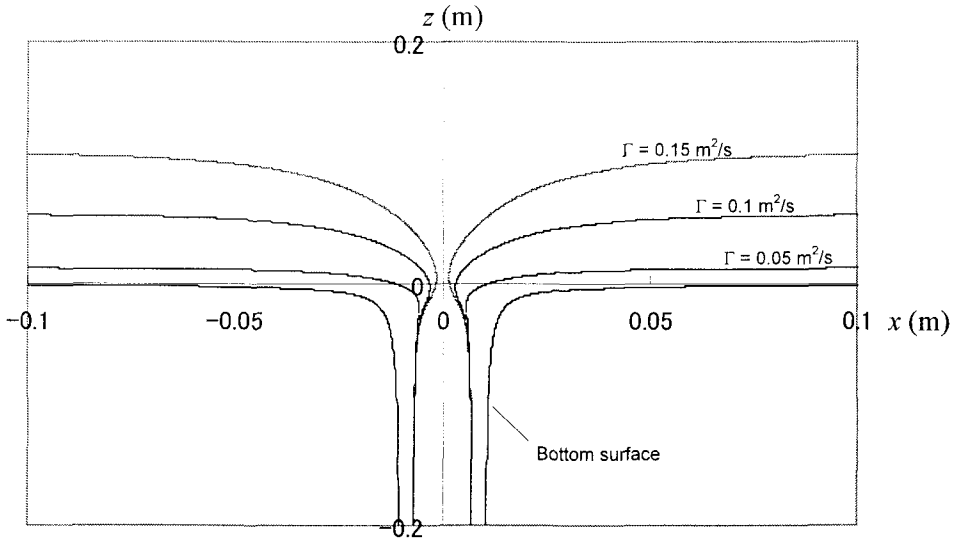

Fig. 5 Different water surface profile with different value of circulation
(a = 0.01m, b = 10^{-4}m^2, Q_0 = 5. 10^{-5} m^3/s, f =0.015)

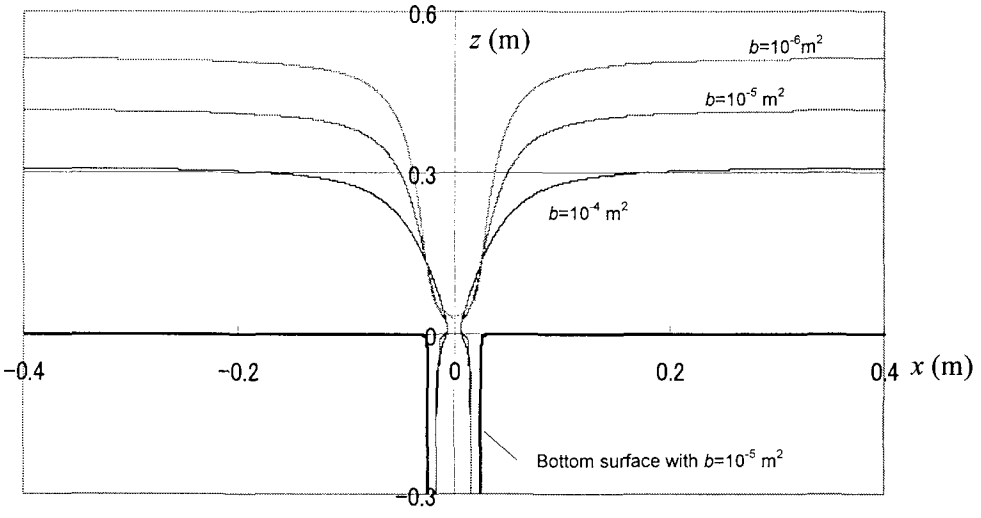

Fig. 6 Changing of water surface profile with different shape of bottom
(a = 0.025m, Q_0 = 5. 10^{-5} m^3/s, Γ=0.4m^2/s, f =0.015)

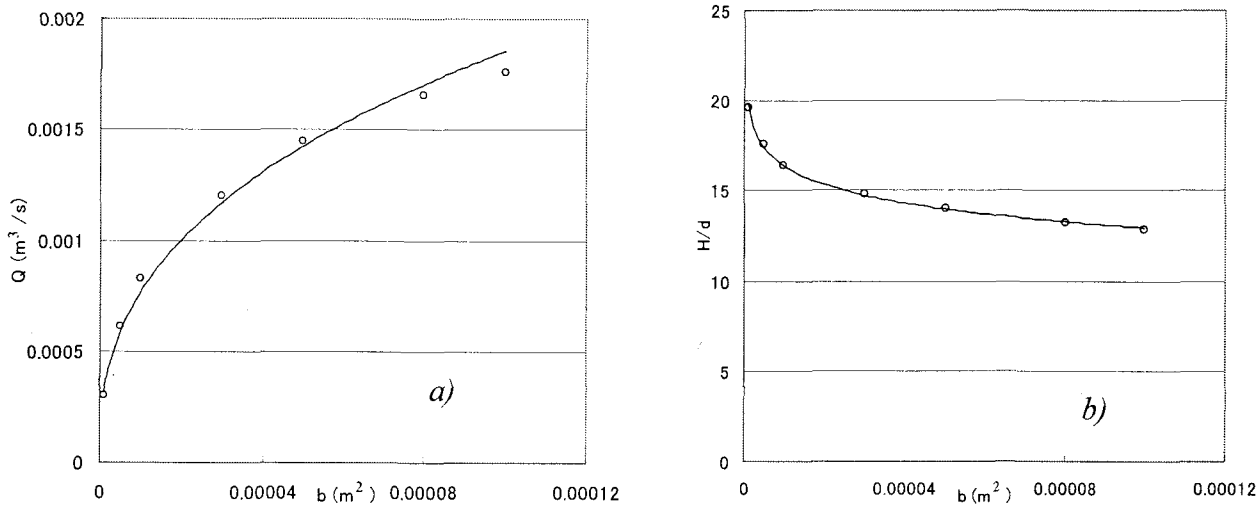

Fig. 7 The effects of value of b on discharge (7*a*) and submergence (7*b*) at an intake

The results also showed that for small decrease in submergence the air core became larger (Fig. 5) that was consistent with Anwar et al's study [4]. From Fig. 5, it was noted that when the circulation increase, the submergence would increase to maintain intake discharge. Hence, the model has the applicability in representing the effects of circulation on the flow through vertical intake.

The effects of intake's shape were examined by changing the value of 'b' in eq. (3). In these cases, three simulations were considered with value of b = 10^{-4}, 10^{-5} and 10^{-6}m^2 while maintaining the value of 'a' at 0.025 m. It can be seen from Fig. 6 that the water depth increased when the intake entrance became sharper (decrease value of b). For more clarity, the computation has been done with the same intake and circulation to test the effects of value of b on intake discharge with unchanged submergence (Fig. 7a) and on submergence with same discharge (Fig. 7b). This phenomenon is in agreement with the physical meaning of the coefficient 'b' and it also improves the effective performance of bellmouth intake.

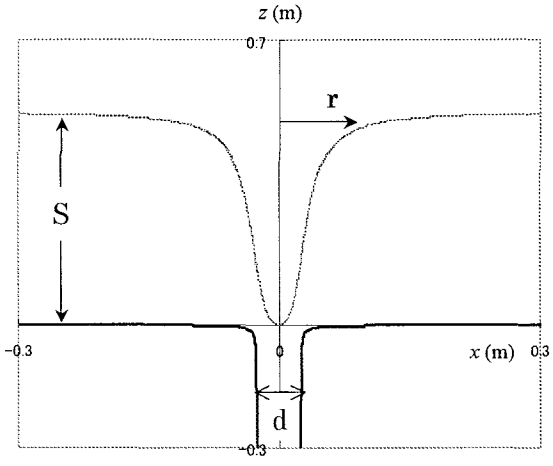

Fig. 8 Definition sketch of critical submergence

The model also can be used to predict the critical submergence which has been defined as the submergence when the tip of air core vortex just reaches the intake (Fig 8). A large quantity of experimental data has been used in Odgaard's study [2] to verify the equation presenting critical submergence in the absence of surface tension (eq. 18 in [2]):

$$\frac{S}{d} = \frac{R_e}{23.2} 5.6\left[N(\Gamma)\right]^{0.5} Fr^{0.5} \qquad (26)$$

where circulation function $N(\Gamma) = \frac{S\Gamma}{Q_0}$, Froude number $Fr = \frac{V}{(gd)^{1/2}}$ and Reynold number $\mathrm{Re} = \frac{Q}{\upsilon d}$.

This equation can be applied for the case of vortex with turbulent core with υ replaced by $\upsilon + k\Gamma$. From calibration the value of k was then estimated to be $k \approx 6\times10^{-5}$.

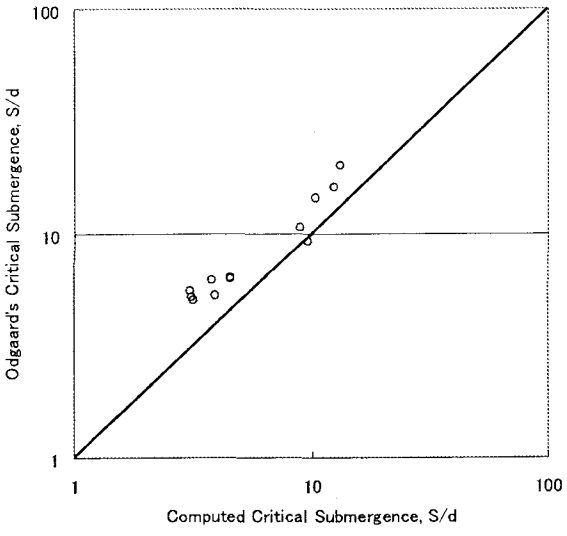

Fig. 9 Comparison of computed critical submergence by model (eq. 23) and by Odgaard's equation (eq. 26)

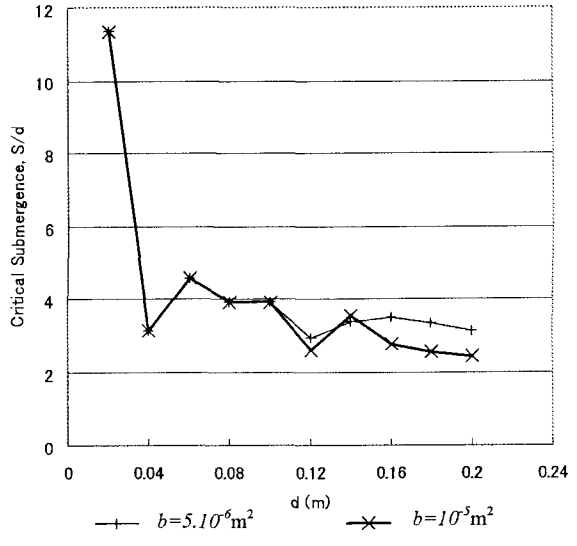

Fig. 10 The variation of critical submergence with different values of b

A total of 12 simulations were made with b=10^{-5}m^2 and all the range of intake diameter from 0.01 to 0.2m. The comparison of computed critical submergences by the model and by Odgaard's equation (eq. 26) is showed

in Fig. 9. The horizontal coordinate is the computed critical submergences by the present model and vertical coordinate is by Odgaard's. The perfect fit between model and Odgaard's equation is on the 45° line. It can be seen from the figure that there was a good agreement, thus the model can be used to predict critical submergence of a vertical intake.

Fig. 10 shows the variation of critical submergence with different value of b (for each case, intake's diameter and discharge were kept constant). It is observed from the figure that the critical submergence was not significantly affected by a small change of b with order of $10^{-5}m^2$.

5. Conclusions

A 1D theoretical model based on the depth-averaged and momentum equations has been developed to calculate the variation of water depth of flow with air-core vortex at an intake. Hence, the water surface profile can be directly derived from the model. The use of curvilinear coordinate avoids invalidation of the Kelvin's theorem in the core of vortex, thus the conservation of circulation can be applied for whole flow.

The comparison of calculated data by the model and an empirical equation shows that the proposed model yields reliable results in predicting the critical submergence of the intake without any limitation of Froude number - a problem that most of existing model cannot escape. It is expected that the model can be improved to unsteady case in follow-up paper.

References

1. Jain S. C.: Tangential vortex-inlet, *J. Hydr. Eng. ASCE*, Vol. 110, No. 12, pp.1693-1699, 1984
2. Odgaard A. J.: Free-surface air core vortex, *J. Hydr. Eng. ASCE*, Vol. 112, No. 7, pp.610-620, 1986
3. Hite J. E. and Mih C. W.: Velocity of air core vortices at hydraulic intakes, *J. Hydr. Eng. ASCE*, Vol. 120, No. 3, pp.284-297, 1994
4. Anwar O. H., Weller A. J. and Amphlett B. M.: Similarity of free-vortex at horizontal intake, *J. Hydr. Res.*, Vol. 16, No. 2, 1978
5. Jain A. K., Raju K. G. R. and Garde R. J.: Vortex formation at vertical pipe intake, *J. Hydr. Div. ASCE*, Vol. 104, No. 10, pp.1429-1445, 1978
6. Yıldırım N. and Kocabas F.: Critical submergence for intakes in open channel flow, *J. Hydr. Eng., ASCE*, Vol. 121, No.12, pp 900–905, 1995.
7. Yıldırım N. and Kocabas F.: Closure to 'Critical submergence for intakes in open channel flow, *J. Hydr. Eng., ASCE*, Vol. 123, No. 6, pp 589–590, 1997
8. Yıldırım N. and Kocabas F.: Critical submergence for intakes in still-water reservoir, *J. Hydr. Eng., ASCE*, Vol. 124, No. 1, pp. 103–104, 1998
9. Trivellato F., Bertolazzi abd Firmani B.: Finite volume modeling of free surface draining vortices, *J. Comp. App. Mech.*, Vol. 103, pp. 175-185, 1999
10. Posey C. J. and Hsu H.: How the vortex affects orifice discharge, *Engineering News Record*, Vol. 144, p. 30, 1950

(Received: April 16, 2004)